Thermochimica Acta, 54 (1982) 71–85
Elsevier Scientific Publishing Company, Amsterdam—Printed in The Netherlands

ON THE VALIDITY OF A FIRST-ORDER KINETICS SCHEME FOR THE THERMAL DECOMPOSITION OF OIL SHALE KEROGEN

K. RAJESHWAR * and J. DUBOW

Department of Electrical Engineering, Colorado State University, Fort Collins, CO 80523 (U.S.A.)

(Received 10 September 1981)

ABSTRACT

Kinetics data from a previous study on the thermal decomposition of Green River oil shale kerogen were reanalyzed in terms of topochemical models conventionally employed for solid-state reactions. The analyses revealed that the thermal decomposition proceeded by mechanisms which were more complex than the simple first-order rate law proposed by previous authors. The reactant/product interface and effects arising from diffusion of product gases from the oil shale matrix played a key role in the kinetics of the decomposition reaction. The decomposition mechanism was seen to switch from simple first-order at low temperatures ($\leq$400°C) to phase-boundary controlled at intermediate temperatures (400–450°C). The reaction became strongly diffusion-controlled at temperatures above 450°C. There was also evidence for zero-order kinetics in some cases. A sensitivity analysis, however, revealed that effective or procedural kinetics parameters could be extracted such that the magnitude of these parameters was relatively insensitive to the particular kinetics model employed. These global kinetics parameters may have relevance to practical applications such as those related to modeling of retort processes. A rate expression given by $k = 3.69 \times 10^{11} \exp(-21059/T)$ (min^{-1}) was deduced for the high temperature stage in the decomposition associated with the conversion of pyrolytic bitumen to the final products.

INTRODUCTION

Much attention has been focused in recent years on the kinetics of the thermal decomposition of oil shale kerogen (for a review of previous work on this topic, see ref. 1). Impetus for these studies derives largely from the relevance of kinetics data to design of oil shale retorting schemes. Both isothermal [2–5] and non-isothermal [4,6] techniques have been employed to study the decomposition kinetics and their relative merits discussed [4]. A variety of reaction schemes ranging in complexity from simple first order [2–6] to a set of seventeen competing reactions [7], have been proposed to explain the observed trends. The serious discrepancies between the various values reported in the literature for the kinetics parameters combined with the extreme sensitivity of the decomposition reaction to experimental conditions [1], seem to suggest that the thermal decomposition of oil shale kerogen is more complex than the behavior predicted by a first-order kinetics scheme. Attempts have been

* To whom correspondence should be addressed.

0040-6031/82/0000–0000/$02.75

made, therefore, by previous authors to describe this reaction by a second-order (non-linear) kinetics model [8,9]. This approach has two difficulties: (a) detailed considerations [10] show that only values of reaction order equal to 0, 1/2, 2/3 or 1 have theoretical justification for decomposition reactions in the solid state [11], and (b) the concept of reaction order in solid-state decomposition reactions assumes a significance which is completely different from that adopted in homogeneous reaction kinetics [6]. The kinetic order for reactions in the solid state merely describes topochemical aspects at the reactant/product interface. An alternative explanation must therefore be sought to rationalize the complexities observed in the decomposition kinetics of oil shale kerogen. In a previous article [1], we had proposed that diffusion of product gases from the oil shale matrix may play an increasingly important role in the decomposition kinetics especially at elevated temperatures (>450°C). In this regard, it was pertinent to note the findings of previous authors [12] that most observations of first-order kinetics could be reinterpreted in terms of a diffusion-controlled mechanism. Precedence for observation of diffusion-control in oil-shale pyrolysis may be found in an earlier work [13] although the effects were not evaluated in a quantitative fashion. We were prompted, therefore, to re-examine the earlier kinetics data on the thermal decomposition of oil shale kerogen in the light of existing models for decomposition reactions in the solid state. Kinetics data for the present analyses were taken from the pioneering work of Hubbard and Robinson [3].

ANALYTICAL PROCEDURES

Hubbard and Robinson [3] present data showing the variation in the fraction of kerogen decomposed (α) with the time of heating (t') for temperatures ranging from 350 to 525°C. Three shale samples from the Green River formation with oil yields ranging from 108 l tonne^{-1} to 300 l tonne^{-1} were examined. In isothermal experiments such as those employed by Hubbard and Robinson [3], it is difficult to obtain the chosen reaction temperature instantaneously and hence to define a zero time for the reaction. This problem becomes more severe at elevated temperatures because the time required to attain the isothermal temperature becomes a large fraction of the total reaction period [1]. No corrections for zero time were employed by Hubbard and Robinson in their kinetics analyses, although Braun and Rothman [14] later modified the Hubbard and Robinson data with the inclusion of an "induction period" to take into account the effect of heat-up times. The following procedure was adopted in the present study for kinetics analyses: The "raw" data of Hubbard and Robinson were fitted by regression analyses to yield a set of α vs. t' curves at the various temperatures for each shale sample. Typical curves are illustrated in Fig. 1. The displacement of these curves from the origin corresponding to zero time in these plots was taken as an effective measure of t_0, the time required for the sample to attain the isothermal reaction temperature. The reaction times (t) were then obtained as $t = t' - t_0$. All subsequent kinetics analyses were carried out on α vs. t data.

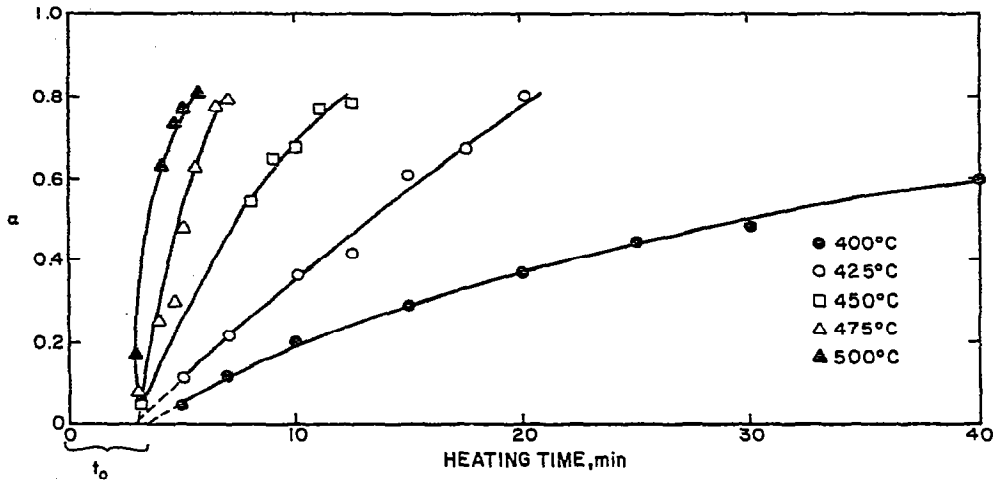

Fig. 1. Representative plots of the fractional conversion (α) of oil shale kerogen vs. heating time.

The t_0 values were usually dependent on temperature and also showed minor variations with the oil yield of the shales. The values ranged in magnitude from 3 min for the 108 l tonne^{-1} sample to 8 min for the 300 l tonne^{-1} sample at 425°C.

The data of Hubbard and Robinson at the extreme ends of their temperature range were omitted for the present study because: (a) at elevated temperatures (> 500°C), the total reaction period was extremely short (< 5 min) and consequently the heat-up time occupied a significant fraction of the reaction period. The errors thereby introduced in the kinetics data are likely to be large (vide supra); (b) at the lower end of the temperature range (< 375°C), the range of α values available for kinetics analyses was restricted because of the exceedingly slow rate of the decomposition reaction.

As outlined below, the α vs. t data were subsequently processed in terms of kinetics models conventionally adopted for reactions in the solid state.

RESULTS AND DISCUSSION

A general equation describing the kinetics of reactions in condensed phases is [15]

$$\alpha = 1 - \exp(-Bt^m) \tag{1}$$

or

$$-\ln \ln(1-\alpha) = \ln B + m \ln t \tag{2}$$

where B is a constant which depends in part on the vibration frequency and of the linear rate of grain growth and m is a constant which can vary according to the reaction mechanism. According to eqn. (2), $-\ln \ln(1-\alpha)$ when plotted against $\ln t$ should yield a straight line with slope m. Theoretical values of m corresponding to a particular decomposition mechanism have been tabulated by previous authors [15].

Diffusion-controlled decomposition mechanisms yield m values between 0.54 and 0.62, a first-order reaction gives a slope of unity, phase-boundary controlled reactions are characterized by m values of either 1.07 or 1.11 depending on the geometry and the Avrami–Erofeev (nucleation and growth) reactions yield m values of 2 and 3, the values again depending on the specific geometry of the reactant/product interface. Although the inherent accuracy in α vs. t data is usually insufficient to distinguish between the exact mechanisms comprising the above broad classes of reactions (e.g. below the two sub-classes of phase-boundary controlled reactions, contracting cylinder: $m = 1.07$ and contracting sphere: $m = 1.11$), the magnitude of the slopes are sufficiently different between major categories of reaction models to enable preliminary identification at the onset of a kinetics analysis. Subsequent differentiation may be achieved by supportive information on the specific reaction geometry and sample shape employed and also by plotting the functions corresponding to a specific model versus t over a wide range of α (vide infra). The functions usually adopted for reaction kinetics in the solid-state are described in refs. 16 and 17. It is pertinent to note that in the above method of analyzing isothermal kinetics data, errors due to heat-up time and consequent uncertainty in the initial conditions may be avoided by choosing α values above ~ 0.10.

Table 1 lists the m values obtained for the three Green River oil shale samples studied by Hubbard and Robinson. The variation of m with temperature is also shown in this table. Representative plots of $-\ln \ln(1-\alpha)$ vs. t from which values of m were obtained (cf. eqn. (2)) are shown in Fig. 2. Three points may be noted in the data shown in Table 1: (a) the slopes differ significantly from unity for all the three samples. This immediately suggests that the decomposition of oil shale kerogen does not follow a simple first-order law; (b) the m values are significantly low at temperatures $> \sim 425$°C. Such low values would be consistent with a situation where product diffusion starts to exercise greater control on the overall kinetics at elevated temperatures where the reaction rates are intrinsically high. Compelling proof that this is indeed so is provided by the analyses below, and (c) the thermal decomposition of oil shale kerogen is kinetically complex and no single model describes adequately the behavior over the entire temperature range from 375 to 500°C. For example, apart from diffusion-controlled mechanisms at temperatures above ~ 475°C, there is evidence for phase-boundary controlled kinetics behavior at intermediate temperatures (e.g. at 450°C for the 212 l tonne^{-1} sample). A zero order reaction mechanism ($m = 1.24$) would be also consistent with the data at specific temperatures (e.g. 425°C, Table 1) for the three samples. Further evidence for zero-order rate law is provided by the almost linear nature of the α vs. t curves at this temperature (cf. Fig. 1).

It is pertinent to note at this point that Hubbard and Robinson had analyzed their kinetics data in terms of first-order kinetics. In fact, with the exceptions noted above in the introductory paragraph, a first-order model seems to be the one favored by most authors in studies on oil shale.

Another method of analyzing the kinetics of condensed phase reactions makes use of reduced-time plots [17]. This method is based on the validity of a general

TABLE I

Characteristic slopes [cf. eqn. (2)] and kinetics rate constants for Green River oil shale

Oil yield (l tonne^{-1})	Kinetics parameter	Temperature (°C)					
		375	400	425	450	475	500
108	m [a]		0.83	1.28	0.89	0.81	0.52
	k_1 (min^{-1}) [b]		0.26×10^{-1}	0.67×10^{-1}	0.16	0.40	0.95
	k_2 (min^{-1})		0.14×10^{-1}	0.29×10^{-1}	0.07	0.15	0.36
	k_3 (min^{-1})		0.90×10^{-2}	0.21×10^{-1}	0.46×10^{-1}	0.11	0.29
212	m	0.96	0.90	1.22	1.10	0.85	
	k_1 (min^{-1})	0.34×10^{-2}	0.17×10^{-1}	0.53×10^{-1}	0.13	0.65	
	k_2 (min^{-1})	0.16×10^{-2}	0.75×10^{-2}	0.24×10^{-1}	0.53×10^{-1}	0.27	
	k_3 (min^{-1})	0.11×10^{-2}	0.55×10^{-2}	1.70×10^{-2}	4.35×10^{-2}	0.20	
300	m		0.92	1.23	1.32	0.68	0.74
	k_1 (min^{-1})		0.13×10^{-1}	0.71×10^{-1}	0.11	0.43	
	k_2 (min^{-1})		0.06×10^{-1}	0.32×10^{-1}	0.05	0.16	
	k_3 (min^{-1})		0.43×10^{-2}	0.23×10^{-1}	0.36×10^{-1}	0.11	

[a] Slopes extracted from plots of $-\ln\ln(1-\alpha)$ vs. $\ln t$ (cf. Fig. 2).

[b] k_1, k_2 and k_3 correspond to rate constants in eqns. (5)–(7), respectively (see text).

[c] The rate constant for the contracting-cylinder and controlling sphere equations is given by $k=u/r$ where u is the velocity of movement of the reactant/product interface and r is the sample radius (ref. 17). Hubbard and Robinson used oil shale cylinders of radius 1 cm. The above expression in this case therefore reduces to $k=u$ (min^{-1}).

expression of the form

$$F(\alpha) = kt \tag{3}$$

where $F(\alpha)$ is a function describing the reaction mechanism and k is the rate

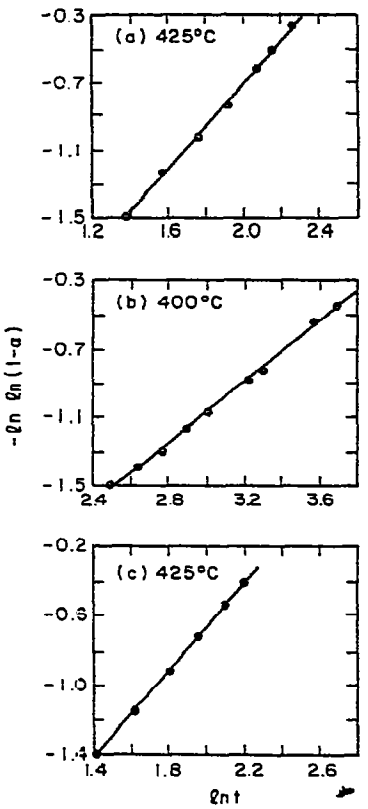

Fig. 2. Plots of $-\ln \ln(1-\alpha)$ vs. $\ln t$ (eqn. (2)) for Green River oil shale kerogen: (a) 108 l tonne^{-1} sample, 425°C; (b) 212 l tonne^{-1} sample, 400°C; (c) 300 l tonne^{-1} sample, 425°C.

constant at a given temperature. On a reduced time scale the above expression reduced to

$$F(\alpha) = A(t/t_{0.5}) \tag{4}$$

where $t_{0.5}$ is the time at which $\alpha = 0.5$ and A is a calculable constant which depends on the form of $F(\alpha)$. The advantage of the approach based on reduced-time plots is that a single curve can be calculated of α vs. $(t/t_{0.5})$ for a particular kinetics model. This curve may then be directly compared with experimental data for all values of temperature, pressure and other variables for which eqn. (3) remains valid. Therefore, any change in the kinetics and mechanism over the range of temperatures selected for the reaction under investigation, may be readily identified. Conversely, a reaction which obeys a single kinetics model throughout the temperature range of study, would yield experimental data which are described by a single α vs. $t/t_{0.5}$ curve [17].

Figure 3 illustrates reduced-time plots for the 108 l tonne^{-1} oil shale sample. Figures 4 and 5 illustrate corresponding data on the 212 and 300 l tonne^{-1} samples. Also shown for comparison are the "theoretical" α vs. $t/t_{0.5}$ curves for first-order kinetics, diffusion-controlled reaction in a sphere or cylinder and a contracting sphere and cylinder (phase-boundary controlled) decomposition model. The results shown in Figs. 3–5 are entirely consistent with the trends observed from the preceding analysis (cf. Table 1). Agreement with a diffusion-controlled reaction model is particularly good at elevated temperatures (e.g. 500°C) for the 108 and 300 l tonne^{-1} samples and is consistent with the low m values observed at these temperatures (Table 1). Differentiation between a first-order model and the phase-boundary controlled reaction mechanisms seems to be less clear-cut in the data shown in Figs. 3–5 except perhaps at high conversions. This difficulty as stated above, is fairly common in analyses of solid-state kinetics. While major categories of reaction mechanisms may be readily distinguished, differentiation between the behavior shown by differing geometries within the confines of a particular kinetic model is difficult. In any case, as shown by the results of the preceding analyses, it is unlikely at least under the conditions employed by Hubbard and Robinson [3], that any one single model adequately represents oil shale decomposition kinetics throughout the temperature range 375–500°C. Two points clearly emerge from the data described thus far: (a) diffusion-control becomes increasingly important at elevated temperatures ($>\sim 475$°C), (b) the kinetics behavior is extremely sensitive to the sample geometry and experimental conditions such that any significance attached to the kinetics parameters thereby extracted must take these complicating factors into account.

It seems pertinent at this point to ask the question "Can meaningful values of kinetics parameters be extracted in spite of the complexities noted above in the

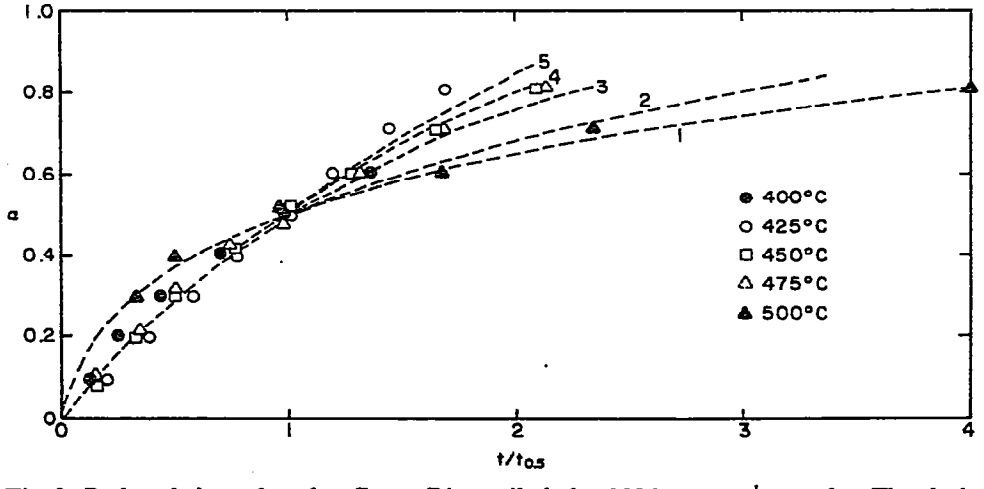

Fig. 3. Reduced-time plots for Green River oil shale (108 l tonne^{-1} sample). The dashed lines marked 1–5 represent the theoretical curves for diffusion-controlled reactions in a sphere and cylinder first-order reaction and phase-boundary controlled reactions in a contracting sphere and cylinder, respectively (cf. ref. 17).

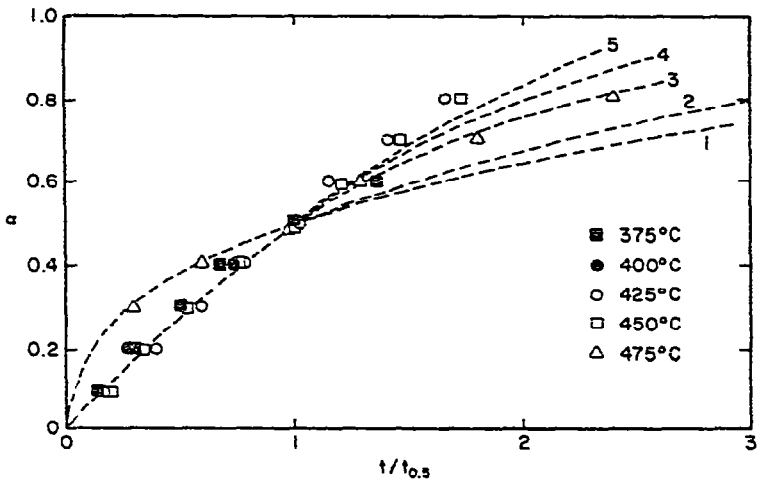

Fig. 4. Reduced-time plots for Green River oil shale (212 l tonne^{-1} sample). The dashed lines correspond to notation in Fig. 3.

mechanistic aspects of the decomposition reaction?". To address this question, we employ a criterion wherein we examine the extent of sensitivity of the computed kinetics parameters to the particular model (vide supra) chosen for the analysis. If the parameters show drastic variations depending on the model employed, then their usefulness is questionable. Conversely, if the parameters are relatively insensitive to the particular kinetics model chosen for their computation, then a "global" kinetics representation may be employed to describe the overall decomposition reaction. Such a representation may have relevance to practical applications such as those related to modeling of oil shale retorts.

For this purpose, the α vs. t data for the three oil shale samples were re-analyzed

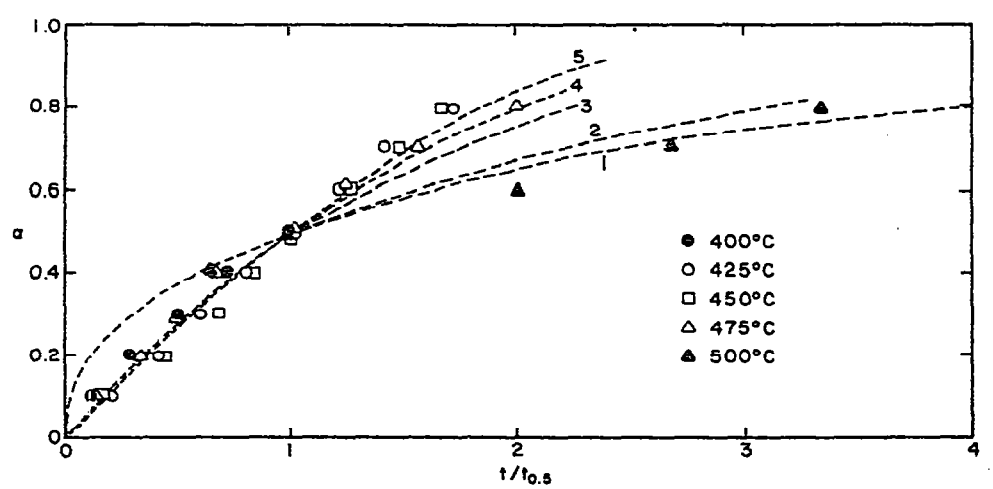

Fig. 5. Reduced-time plots for Green River oil shale (300 l tonne^{-1} sample. The dashed lines correspond to notation in Fig. 3.

in terms of F(α) vs. t plots for a first-order model and phase-boundary controlled reaction mechanisms. Two separate models for the latter were employed based on a contracting cylinder and a contracting sphere geometry. The relevant equations for the kinetics models are respectively [16,17]

$$-\ln(1-\alpha) = k_1 t \tag{5}$$

$$1-(1-\alpha)^{1/2} = k_2 t \tag{6}$$

$$1-(1-\alpha)^{1/3} = k_3 t \tag{7}$$

Representative plots are shown in Figs. 6–8 for the data at various reaction temperatures on the 212 l tonne^{-1} sample. Similar plots were obtained for the 108 and 300 l tonne^{-1} samples. From the slopes of these straight-line plots, the rate constants for the three mechanisms were extracted at different temperatures [cf eqns. (5)–(7)]. These are tabulated in Table 1.

The rate constants are related to temperature by the Arrhenius expression

$$k = A \exp(-E_a/RT) \tag{8}$$

where A is the pre-exponential factor, E_a is the activation energy, R is the universal gas constant and T is the absolute temperature. According to eqn. (8), plots of ln k vs. $1/T$ should yield straight lines from which the kinetics parameters A and E may be extracted from the intercept and slope, respectively. Figures 9–11 illustrate Arrhenius plots obtained for the three Green River oil shale samples. The kinetics parameters extracted by least-square analyses of the data in Figs. 9–11 are assembled in Table 2.

The following points may be noted in the data in Figs. 9–11 and Table 2: (a) both the first-order rate law [eqn. (5)] and the contracting-interface expressions [eqns. (6)

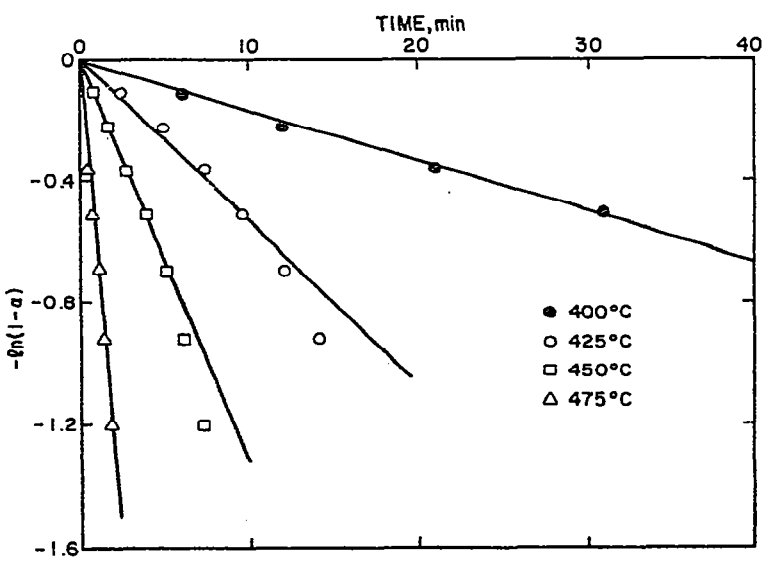

Fig. 6. Plots of the first-order equation [eqn. (5)] for Green River oil shale (212 l tonne^{-1} sample). Temperature is shown as the parameter.

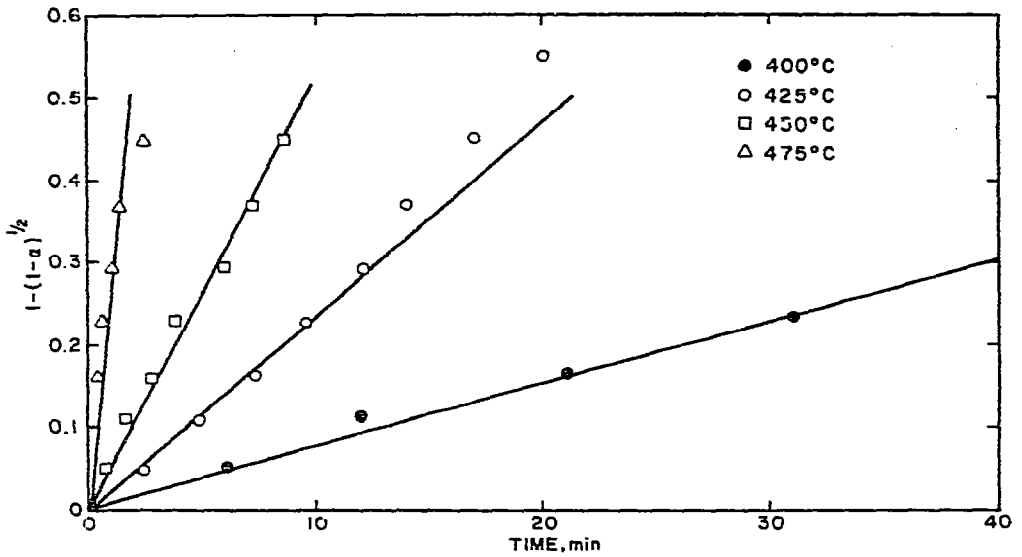

Fig. 7. Plots of the contracting-sphere equation [eqn. (6)] for Green River oil shale (212 l tonne^{-1} sample). Temperature is shown as the parameter.

and (7)] yield kinetics parameters which are essentially the same within the limits of experimental and analytical errors; (b) the magnitude of the kinetics parameters does not show a systematic dependence on the oil yield of the shale. Hubbard and Robinson [3] came to a similar conclusion from analyses of their kinetics data; (c) the pyrolysis of oil shale kerogen is described by a single reaction over the temperature range 375–500°C. The break at ~437°C observed by Hubbard and Robinson in their Arrhenius plots is absent in the present data for all three samples (Figs. 9–11), and (d) values of E_a obtained in the present study are significantly different from those obtained by Hubbard and Robinson using a first-order kinetics

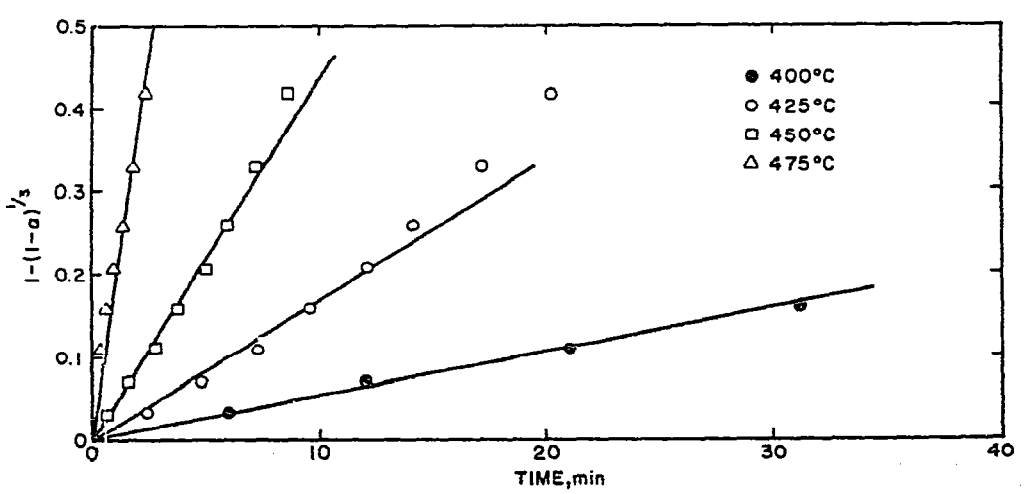

Fig. 8. Plots of the contracting-cylinder equation [eqn. (7)] for Green River oil shale (212 l tonne^{-1} sample). Temperature is shown as the parameter.

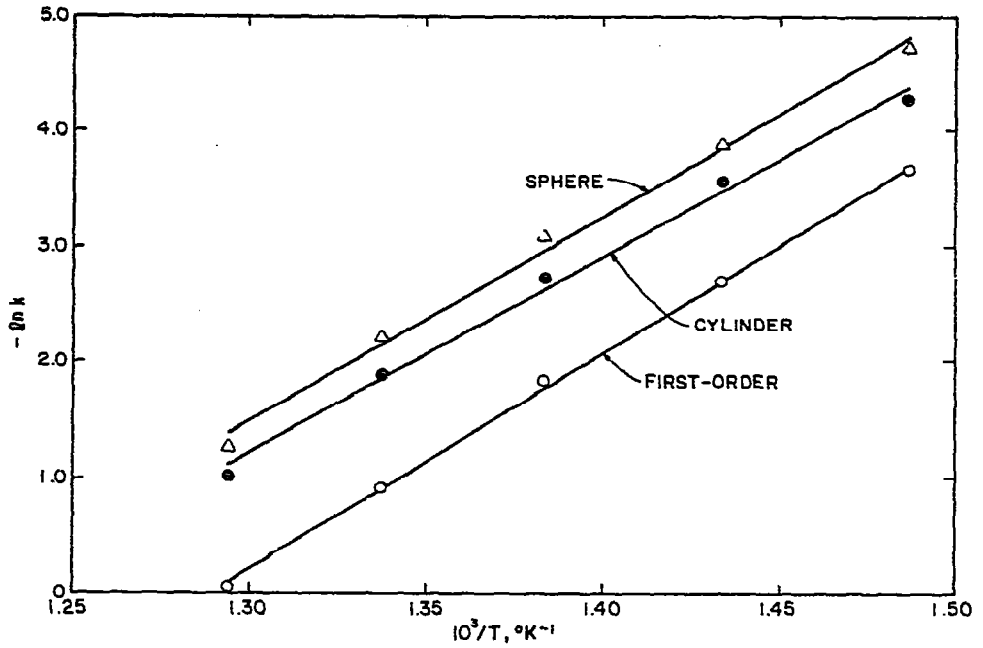

Fig. 9. Arrhenius plots for Green River oil shale (108 l tonne^{-1} sample). The symbols (○), (●) and (△) denote rate constants calculated from eqns. (5)–(7), respectively.

model (113.72 kJ mole^{-1} below 437°C and 46.51 kJ mole^{-1} above 437°C).

The relative insensitivity of the kinetics parameters to the particular model chosen for the analyses is encouraging from an applications viewpoint and suggests that

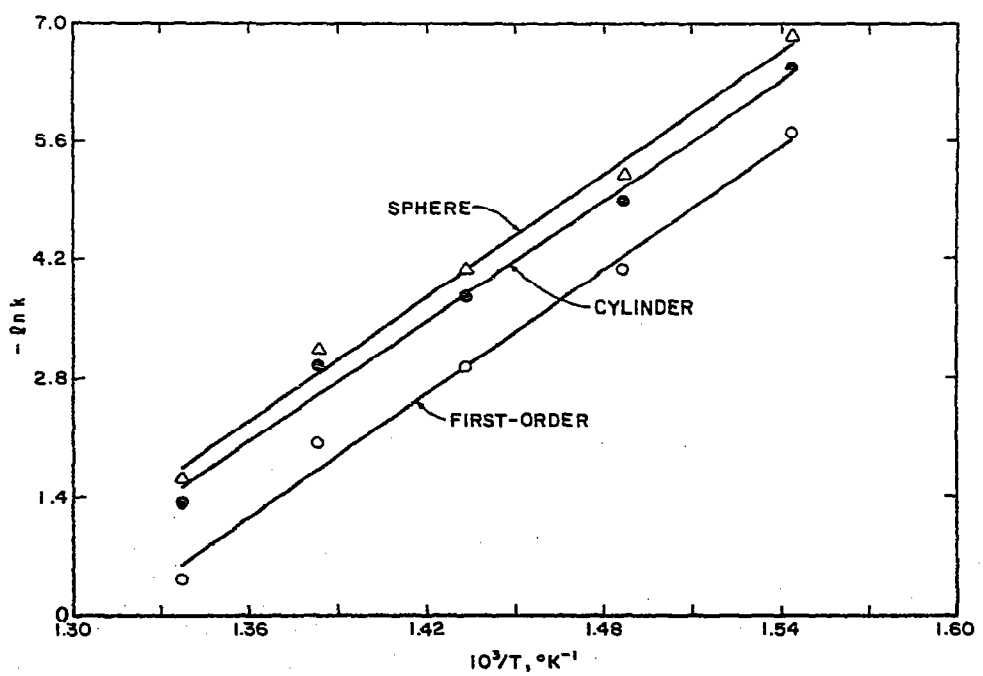

Fig. 10. Arrhenius plots for Green River oil shale (212 l tonne^{-1} sample). Notation as in Fig. 9.

TABLE 2

Kinetics parameters for the thermal decomposition of Green River oil shale kerogen

Oil yield (l tonne^{-1})	Kinetics parameters [a]								
	First-order equation			Contracting-sphere equation			Contracting-cylinder equation		
	ln A	A (min^{-1})	E_a (kJ mole^{-1})	ln A	A (min^{-1})	E_a (kJ mole^{-1})	ln A	A (min^{-1})	E_a (kJ mole^{-1})
108	24.2	3.24×10^{10}	157.54	21.7	2.66×10^{9}	149.16	20.86	1.15×10^{9}	142.38
	(0.4)		(2.10)	(0.9)		(5.03)	(0.9)		(4.86)
212	32.0	7.90×10^{13}	204.47	30.8	2.38×10^{13}	204.47	30.23	1.34×10^{13}	198.94
	(1.7)		(8.97)	(1.6)		(8.97)	(1.9)		(9.97)
300	28.4	2.15×10^{12}	183.52	25.4	1.07×10^{11}	172.63	26.14	2.25×10^{11}	175.14
	(3.5)		(18.02)	(3.4)		(17.51)	(3.2)		(16.51)
Average	28.2	1.77×10^{12}	181.84	26.0	1.89×10^{11}	175.42	25.7	1.45×10^{11}	172.15

[a] Values shown in parentheses are standard deviations calculated by least-squares analyses.

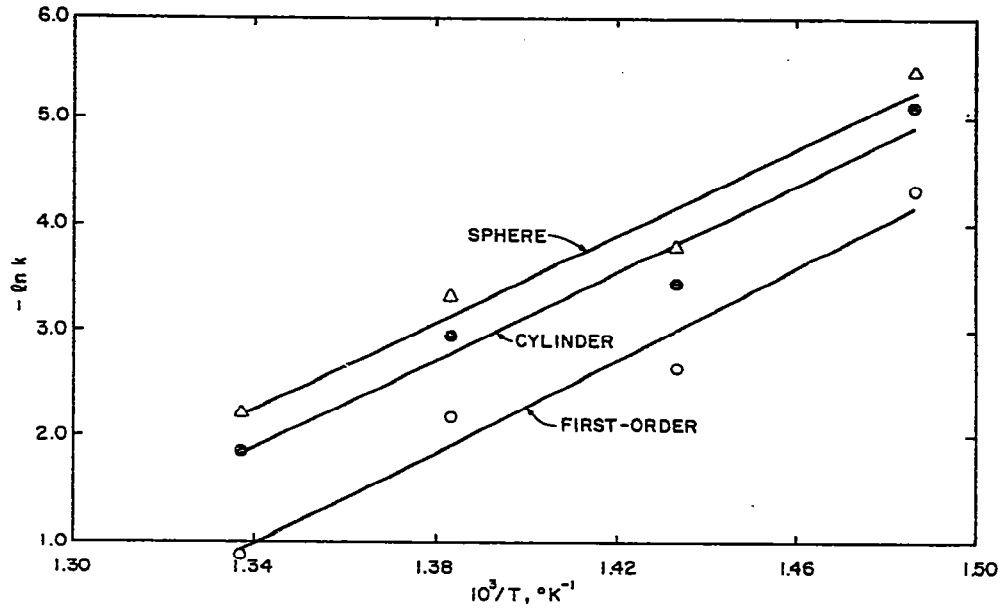

Fig. 11. Arrhenius plots for Green River oil shale (300 l tonne^{-1} sample). Notation as in Fig. 9.

meaningful values of kinetics parameters may be extracted in spite of the complexities noted above in the detailed mechanistic aspects of the decomposition reaction. However, it is reiterated that such values are only "effective" or "procedural" in that any further interpretation of these parameters in terms of chemical or structural alterations undergone by oil shale kerogen, must take into account the complex topochemistry of the reactant/product interface (vide supra).

Unlike our previous study [6] on the thermal decomposition kinetics of oil shale kerogen under non-isothermal conditions, we have not been able to resolve the low-temperature step associated with the thermal decomposition of kerogen to a bitumen intermediate. The reaction temperatures of Hubbard and Robinson which were included for the present analyses are too high for the low-temperature step to play a predominant role in the overall kinetics [18]. (For the reasons mentioned above, temperatures below 375°C were not included for the present study.) This is confirmed by the location of the break-point (~ 400°C) in the Arrhenius plots at the lowest heating rate employed in the previous study [6]. This "knee' is expected to be shifted to still lower temperatures under isothermal conditions. We do not believe that the break observed by Hubbard and Robinson at 437°C in their Arrhenius plots is associated with the reaction sequence

$$\text{Oil shale kerogen} \xrightarrow{>375^\circ C} \text{pyrolytic bitumen} \xrightarrow{<375^\circ C} \text{gas} + \text{oil} + \text{carbon residue} \qquad (9)$$

On the other hand, the changes in slope observed by these authors in their Arrhenius plots may be attributed to difficulties in measuring decomposition rates and to the complicating effects of heating history (i.e. large heat-up periods, vide supra) at elevated temperatures. The low E_a values (46.51 kJ mole^{-1}) obtained by these

TABLE 3

Comparison of kinetics parameters from the present study[a] with values previously reported in the literature on oil shales

E_a (kJ mole^{-1})	A (min^{-1})	Ref.
176.47	3.69×10^{11}	This work
152.16	6.20×10^{12}	6
217.88	1.80×10^{15}	4
167.60	2.79×10^{13}	2
169.70		5
199.00	4.95×10^{13}	19

[a] Values of E_a and A averaged from those obtained from first-order and contracting-interface equations (cf. Table 2).

authors also reflect the increasing importance of product diffusion and are entirely consistent with the evidence presented above for the onset of a diffusion-controlled reaction mechanism at temperatures above ~475°C.

Finally, Table 3 compares the kinetics parameters obtained from the present analysis with values previously reported in the literature. For this comparison, only the parameters corresponding to the high-temperature step in eqn. (9) have been taken from the available literature data. The spread in the reported values of the kinetics parameters is significantly smaller if the complicating effect of diffusion-control is taken into account. For example, for the comparison shown in Table 3, values of E_a lower than ~80 kJ mole^{-1} have been omitted because we believe, particularly in the light of the present study, that these low E_a values are clouded by artifactual rate-control exercised by diffusion of product gases and therefore do not represent the pyrolysis reaction per se. Therefore, the maximum spread in the E_a values reported in the literature for the high temperature decomposition of oil shale bitumen is only 65.72 kJ mole^{-1} (cf. Table 3) compared with a discrepancy of ~180 kJ mole^{-1} observed in the previous case [1]. The corresponding variation in the pre-exponential factors reflects the rather large errors usually inherent in their computation.

SUMMARY AND CONCLUSIONS

The present study has emphasized the role of the dynamics of the reactant/product interface and diffusion processes in the kinetics of the thermal decomposition of oil shale kerogen. The quantitative aspects of these processes have been established for the first time. The rate-control exercised by heat transfer and product diffusion is likely to be more severe under conditions typical of those existing in above-ground and in-situ oil shale retorts. These effects may be minimized (although admittedly in

an artificial manner) in kinetics studies on oil shale by employing a thin layer of the test sample such that heat and mass transfer is facilitated. A first-order rate law seems to provide a good explanation of the observed kinetics under these conditions [6]. In any event, "global" kinetics parameters may be generated for practical applications related to oil shale retorting such that they describe the overall temperature dependence of the reaction rate rather than the microscopic details associated with the decomposition mechanism.

REFERENCES

1 K. Rajeshwar, N. Nottenberg and J. DuBow, J. Mater. Sci., 14 (1979) 2025
2 C.G. Maier and S.R. Zimmerley, Utah Univ. Res. Invest. Bull., 14 (1924) 62.
3 A.B. Hubbard and W.E. Robinson, U.S. Bur. Mines Rep. Invest., 4744 (1950).
4 J.H. Campbell, G. Koskinas and N. Stout, Lawrence Livermore Lab. Rep. UCRL-52089, 1976 (unpublished).
5 V.D. Allred, Chem. Eng. Prog. Symp. Ser., 62 (1966) 55.
6 K. Rajeshwar, Thermochim. Acta., 45 (1981) 253.
7 A.L. Shul'man and V.A. Proskuryakov, Khim. Tekhnol. Goryuch. Stantsev. Prod. IKh. Pereab., (1968) 278 [as cited in W.F. Johnson et al., Q. Colo. Sch. Mines, 70 (1975) 237].
8 D.W. Fausett, Ph.D. Thesis, University of Wyoming, 1974.
9 D. Finucane, J.H. George and G.H. Harris, Fuel, 56 (1977) 65.
10 A.W. Coats and J.P. Redfern, Nature (London), 201 (1966) 68.
11 It may be argued that the thermal decomposition of oil shale does not strictly proceed in the solid state in view of the nature of the products formed in the reaction and also because of the physical nature of the pyrolytic bitumen intermediate. Adherence of the reaction kinetics to solid-state thermal decomposition models, however, is compelling proof that the process of nucleation, nuclei growth and movement of the reactant/product interface are indeed important (vide infra). Such processes are typical of heterogeneous decomposition reactions (cf. ref. 16).
12 G.W. Brindley, J.H. Sharp, J.H. Patterson and B.N.N. Achar, Amer. Mineral., 52 (1967) 201.
13 A.W. Weitkamp and L.C. Gutberlet, Ind. Eng. Chem., 9 (1970) 386.
14 R.L. Braun and A.J. Rothman, Fuel, 54 (1975) 129.
15 J.D. Hancock and J.H. Sharp, J. Am. Ceram. Soc., 55 (1972) 74.
16 P.W.M. Jacobs and F.C. Tompkins, in W.E. Garner (Ed.), Chemistry of the Solid State, Butterworths, London, 1955, Chap. 7, pp. 184–212.
17 J.H. Sharp, G.W. Brindley and B.N.N. Achar, J. Am. Ceram. Soc., 49 (1966) 379.
18 These authors, in a subsequent study [J.J. Cummins and W.E. Robinson, U.S. Bur. Mines Rep. Invest., 7620 (1972)], report on the rates of product evolution at temperatures in the range 150–350°C. This reaction represents the low-temperature step associated with the conversion of oil shale kerogen to pyrolytic bitumen.
19 S.M. Shih and H.Y. Sohn, Ind. Eng. Chem., Process Des. Dev., 19 (1980) 420.